Thermoelectric properties of $AgGaTe_2$ and related chalcopyrite structure materials

David Parker and David J. Singh
Oak Ridge National Laboratory, 1 Bethel Valley Road, Oak Ridge, Tennessee 37831, USA
(Received 26 January 2012; revised manuscript received 15 March 2012; published 30 March 2012)

We present an analysis of the potential thermoelectric performance of *p*-type $AgGaTe_2$, which has already shown a ZT of 0.8 with partial optimization, and observe that the same band-structure features, such as a mixture of light and heavy bands and isotropic transport, that lead to this good performance are present in certain other ternary chalcopyrite structure semiconductors. We find that optimal performance of $AgGaTe_2$ will be found for hole concentrations between 4×10^{19} and 2×10^{20} cm^{-3} at 900 K, and 2×10^{19} and 10^{20} cm^{-3} at 700 K, and that certain other chalcopyrite semiconductors might show good thermoelectric performance at similar doping ranges and temperatures if not for higher lattice thermal conductivity.

DOI: 10.1103/PhysRevB.85.125209 PACS number(s): 72.20.Pa

I. INTRODUCTION

Thermoelectric performance, as characterized by the so-called figure of merit, ZT, is a property of matter that has attracted much recent interest. The expression for ZT is $ZT = \sigma S^2 T/\kappa$, where S is the thermopower, T is the temperature, σ is the electrical conductivity, and κ is the thermal conductivity, typically written as the sum of lattice and electronic contributions, $\kappa = \kappa_l + \kappa_e$. Obtaining high ZT is a fundamental scientific challenge, since high ZT is a strongly counterindicated transport property. Specifically, one requires (1) high mobility at the same time as low thermal conductivity, suggesting weak scattering of charge carriers, but strong scattering of phonons, (2) high conductivity and high thermopower, (3) low thermal conductivity (i.e., soft lattice) and high melting point, and finally (4) the combination of heavy band behavior (for high S) at the same time as effective controlled doping. Although there is no known fundamental limit on ZT, for many decades the maximum known ZT in any material was near 1.0, while in recent years new concepts such as the use of nanostructuring[1,2] or "rattling"[3–5] to reduce thermal conductivity, and complex or modified electronic structure (e.g., by nanoscale effects,[6] or selection of materials with unusual band structures)[4,7,8] have raised the best ZT values to near 2. Reviews of the field may be found in Refs. 9 and 10.

Here we discuss $AgGaTe_2$ and related chalcopyrite compounds, which we find to have unusual band structures combining heavy and light features that represent one route for resolving the above conundrums, particularly those relating to electrical conductivity and thermopower. An early study of chalcopyrite band structures is found in Ref. 11.

While heavy mass bands are generally favorable toward producing high thermopower, an essential ingredient for thermoelectric performance, such bands also generally reduce the carrier mobility and conductivity, so that very heavy mass bands on their own are not universally beneficial for good thermoelectric performance (i.e., ZT). Light mass bands, by contrast, are favorable for electrical conductivity but not so for thermopower. However, a *mixture* of light and heavy bands has previously been shown to be beneficial for thermoelectric performance,[12] with the light band providing good conduction and the heavy band a small energy scale helpful for the thermopower. The telluride La_3Te_4 is a good example[13] of a high performance material in which this behavior is realized. An explanation of the role of a heavy band–light band mixture in transport is contained in the Appendix.

Combining heavy and light bands near the band edge is one example of a complex band structure affecting transport. As stated above, in general, thermoelectric performance is a counterindicated property, requiring high thermopower (connected with heavy bands) and high mobility (normally associated with light bands). Other examples of complex band structures affecting thermoelectric performance include the complex band structure of Na_xCoO_2 (Refs. 14–16) and the associated "pudding mold" band shape,[17,18] and the modification of band structure by resonant levels.[19]

$AgGaTe_2$ has already shown a ZT of 0.8 at 850 K (Ref. 20) at a low hole doping of approximately 10^{16} cm^{-3}, far outside the heavy doping ranges 10^{19}–10^{21} cm^{-3} where optimal performance is typically found in thermoelectrics. Structurally, it is very different from the chemically related compounds, PbTe and $AgSbTe_2$, as it is tetrahedrally bonded, rather than octahedral. We show that the valence-band electronic structure of this *p*-type material is very similar to that of certain other ternary chalcopyrite semiconductors, which also show two factors favorable for thermoelectric performance—nearly isotropic transport and a mixture of heavy and light bands. The nearly isotropic transport arises from the (well-known) similarity of the chalcopyrite physical structure of these materials and the cubic zinc-blende structure, as described above. We depict the chalcopyrite structure of $AgGaTe_2$ in Fig. 1.

II. MODEL, CALCULATED BAND STRUCTURES, AND DENSITY OF STATES

In order to study the transport in $AgGaTe_2$ and related materials quantitatively, we employ first-principles density-functional theory as implemented in the linearized augmented plane-wave (LAPW) WIEN2K code.[21] Since first-principles methods often significantly understate the band gap, we here employ a modification of the generalized gradient approximation (GGA) due to Tran and Blaha[22] known as a modified Becke Johnson potential,[23] which has been shown to give much more accurate band gaps than the standard GGA. All calculations were performed to self-consistency to an accuracy of better than one meV per unit cell, using

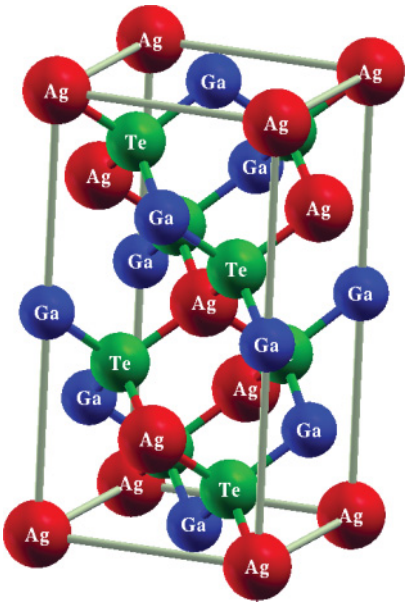

FIG. 1. (Color online) The physical structure of $AgGaTe_2$. The planar lattice constant is 6.23 Å and the c-axis value is 11.96 Å for a c/a ratio of 1.92.

between 1000 and 2000 k points in the full Brillouin zone, with spin-orbit coupling included for all materials except for $ZnSiAs_2$. For $AgGaTe_2$, internal coordinates were optimized, using the Perdew-Burke-Ernzerhof[24] GGA. To calculate the thermopower, as well as the conductivity anisotropy, we used the Boltzmann transport code BOLTZTRAP[25] within the constant scattering time approximation (CSTA). In this approximation, the scattering time of an electron is assumed to depend only on doping and temperature, but not the *energy* of the electron. When employed within the canonical expressions for the thermopower and conductivity, as given in Ref. 26, this results in expressions—the thermopower S and the conductivity anisotropy $\sigma_{\text{planar}}/\sigma_{c\text{-axis}}$—with *no* dependence on any assumed absolute value of the scattering time. The CSTA has been used with quantitative success to describe the thermopower of a large number of thermoelectric materials.[27–36] Its quantitative success is the principal reason for its continued usage, although introducing an energy dependence to the scattering time (as, for example, is theorized to occur with acoustic phonon-electron scattering) would typically have only a minimal decrease on the calculated thermopower. Perhaps the situation wherein the CSTA might be likelier to experience difficulties is in bipolar (double sign) conduction, where the assumption that the valence and conduction bands have equal scattering times can be debated. In such situations, however, thermoelectric performance is typically greatly reduced and so these situations are of little practical interest.

With regard to bipolar conduction, this typically can become an issue when the temperature (literally k_BT, where k_B is Boltzmann's constant) is greater than approximately a sixth of the band-gap value, as noted by Mahan,[37] although this is only a rough qualitative guide; recent work of ours on $CrSi_2$ (Ref. 38) suggests that this material may experience good thermoelectric performance, free from bipolar effects, at temperatures of 1250 K, or roughly a third of the band gap. Clear signatures of bipolar conduction are, for given carrier concentration (as in an experiment), thermopower *decreasing* with increasing temperature. Such a decrease is often accompanied by an *increase* in the electronic component of thermal conductivity which is detrimental to thermoelectric performance. At fixed temperature (as in several of the subsequent plots) a signature of bipolar conduction is a *reduction* in the absolute value of the thermopower with *decreasing* concentration. This is the reverse of the usual situation in which thermopower *increases* with decreasing carrier concentration.

As is well known, in the low-temperature limit the thermopower is proportional to the temperature, which can be seen from the expression for the thermopower [here $\sigma(E)$ is the transport function, $N(E)$, $v(E)$, and $\tau(E)$ are the density of states, Fermi velocity, and scattering time, respectively; f is the Fermi function]

$$S(T) = \frac{\int_{-\infty}^{\infty} dE\sigma(E)(E-\mu)\partial f/\partial dE}{T\int_{-\infty}^{\infty} dE\sigma(E)\partial f/\partial dE}, \quad (1)$$

$$\sigma(E) = N(E)v^2(E)\tau(E). \quad (2)$$

It is clear from Eq. (1) that the thermopower must vanish at $T = 0$, and expansion of the derivative of the Fermi function using the Sommerfeld expansion and an integration by parts yields the T-linear behavior. For higher temperatures the derivative of the Fermi function broadens in energy and the thermopower becomes a complex function of the band structure.

We begin with the band structure, previously considered in Ref. 39. Depicted in Fig. 2 is the calculated band structure of $AgGaTe_2$ within the tetragonal Brillouin zone.[40] The calculated band gap, at 1.15 eV, falls in the center of the 0.9–1.3-eV range of band-gap values found in the literature,[41–48] and is sufficient to prevent bipolar conduction at temperatures of 900 K and below.

Both the valence-band maximum (VBM) and conduction-band minimum (CBM) are located at the Γ point. These pockets generally show a fair degree of isotropy, with the dispersion somewhat greater along the Γ-Z line than the planar

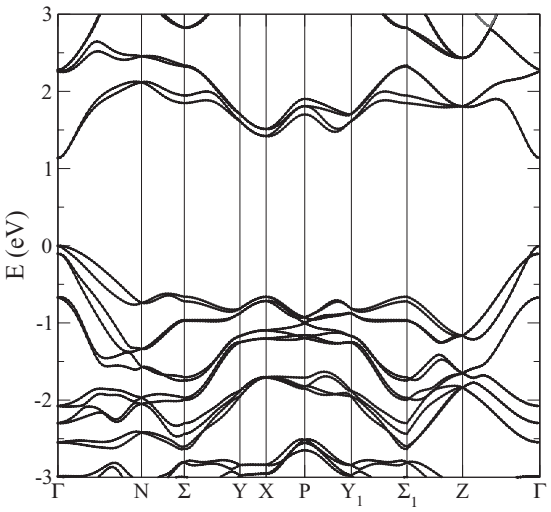

FIG. 2. The calculated band structure of $AgGaTe_2$. The zero of energy is set to the valence-band maximum.

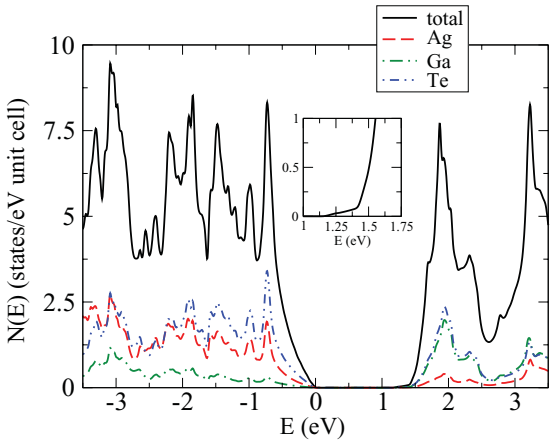

FIG. 3. (Color online) The density of states of $AgGaTe_2$. The zero of energy is set to the valence-band maximum. Inset: the density of states near the conduction-band minimum.

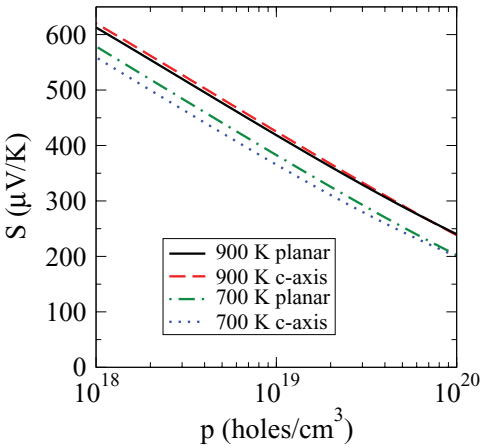

FIG. 4. (Color online) The calculated hole-doped thermopowers of $AgGaTe_2$ at 700 and 900 K.

Γ-N direction. Of interest for the thermoelectric performance, the plot depicts a mixture of heavy and light bands near the VBM. The heavy band shows a Γ-N dispersion of 0.7 eV, leading to an approximate band mass of $1m_0$, with the light band at roughly half this mass. As stated previously, this light band/heavy band combination has previously been shown to be good for thermoelectric performance.[12]

In Fig. 3 we present the calculated density of states. The heavy valence band's impact is immediately apparent, with the DOS rising rapidly just below the VBM. A similarly heavy band appears somewhat above the CBM, with a highly dispersive band (inset) in the first 0.25 eV above the CBM. Also presented in Fig. 3 is the atom-projected DOS. It is worth noting that for all atoms and both the VBM and CBM, the relevant atomic character is of virtually the same shape as the overall DOS, suggesting a coherence to the electronic scattering which tends to affirm the accuracy of the CSTA.

III. CALCULATED THERMOPOWER AND CONDUCTIVITY RESULTS

In Fig. 4 we depict the calculated hole-doped thermopower results for $AgGaTe_2$. The plot depicts (at 700 and 900 K, the maximum operation temperature for $AgGaTe_2$) an essentially logarithmic dependence of thermopower on carrier concentration, in line with Pisarenko behavior. No effects of bipolar conduction are visible, and the plot shows 900-K thermopowers (virtually isotropic as described in Sec. I) approaching 400 μV/K at hole concentrations p of 2×10^{19} cm^{-3}. Given the lack of information regarding the hole mobility at these concentrations and temperatures, estimating the figure of merit ZT at these temperatures is impractical. We can say, however, that in previously studied materials thermoelectric performance is typically optimum for thermopowers between 200 and 300 μV/K. Note that the Wiedemann-Franz relationship implies that, even if the lattice thermal conductivity were nil, a thermopower of 156 μV/K would be required to attain a ZT of unity (the typical minimum value for a material to be considered a "high performance thermoelectric"), so that in practice thermopowers substantially above this value are necessary to achieve high performance.

At 900 K for $AgGaTe_2$ these 200–300-μV/K thermopowers are found for hole concentrations between 4×10^{19} and 2×10^{20} cm^{-3}; at 700 K these thermopowers are found for concentrations between 2×10^{19} and 10^{20} cm^{-3}. While we cannot make a definite estimate of ZT, we can say with high confidence that performance substantially above the $0.8ZT$ value achieved in Ref. 20 will be found. We assert this because the sample in this reference was sufficiently underdoped as to yield a thermopower which *decreased* with increasing temperature from 300 K all the way to the highest temperature measured, strongly indicative of bipolar conduction (always unfavorable for thermoelectric performance). Our results here show that bipolar conduction can be avoided by heavy doping while maintaining high thermopower.

Although experimental work to date has found that $AgGaTe_2$ tends to form p type, in Fig. 5 we present the calculated electron doped thermopower. Somewhat lower values than in the hole-doped case are apparent due to the increased dispersion on the electron-doped side, but the values depicted are still substantial. In addition, as with the valence bands, the conduction bands contain a mixture of heavy and light bands, beneficial for thermoelectric performance. Finally, although the thermopower is lower than for hole doping,

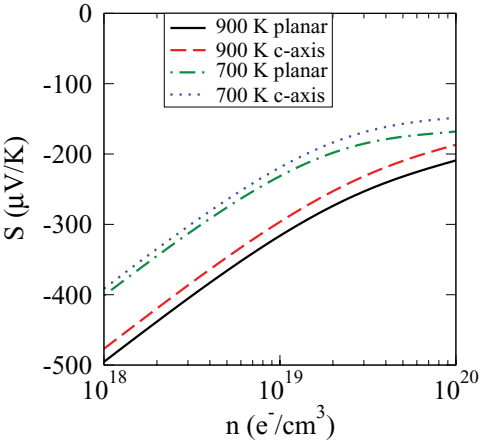

FIG. 5. (Color online) The calculated electron-doped thermopowers of $AgGaTe_2$ at 700 and 900 K.

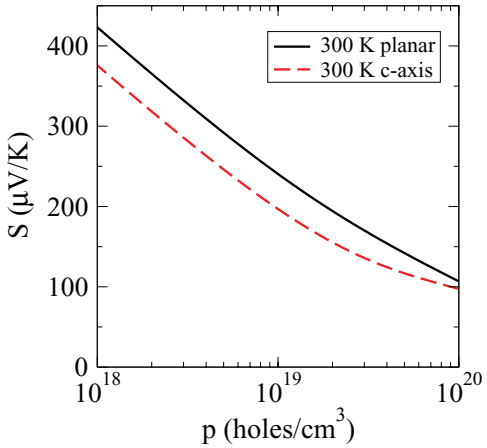

FIG. 6. (Color online) The calculated hole-doped thermopowers of $AgGaTe_2$ at 300 K.

this can be partly compensated for by the likely increased mobility for electron doping. We therefore expect that good performance may obtain for electron doping, in the range of 1.5×10^{19}–10^{20} cm^{-3} at 900 K and 3×10^{18}–2×10^{19} cm^{-3} at 700 K (using the same criteria as for hole doping).

In Fig. 6 we depict the hole-doped thermopower at 300 K. This shows similarly favorable behavior to the high-temperature results, albeit with lower values. Somewhat greater anisotropy than in the high-temperature case is apparent, due mainly to the narrower energy range of the valence band that is relevant for transport at these lower temperatures. This can be seen more directly from looking at the band structure plot (Fig. 2)—the band mass of the light band in the Γ-Z direction is roughly one-half the mass of the heavy band in the Γ-N direction. At low dopings and temperatures (such as 300 K), for c-axis transport it is only this light band that is operative in transport and there is therefore substantial anisotropy in the calculated thermopower. As one moves to heavier dopings the heavier band (whose maximum is roughly 100 meV below the VBM) becomes operative and yields substantially more isotropic behavior. We note also that both planar and c-axis thermopower obey

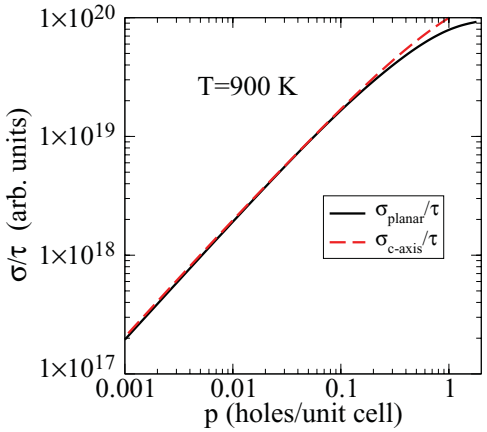

FIG. 7. (Color online) The calculated electrical conductivity (divided by scattering time) of $AgGaTe_2$ at 900 K. Note that one hole per unit cell is equivalent to 4.31×10^{21} cm^{-3}.

a Pisarenko-type relationship (i.e., logarithmic in carrier concentration) at the low dopings, indicative of nondegenerate single band transport, and deviate from this at higher dopings, due both to the two-band behavior and the approaching of the degenerate limit. In Fig. 7 we present the 900-K conductivity anisotropy, which is essentially nil, a significant advantage for applications, as discussed previously.

IV. OBSERVATION ON VALENCE-BAND STRUCTURE IN TERNARY CHALCOPYRITE SEMICONDUCTORS AND THERMOPOWER OF $CdGeAs_2$

In this section we point out that there are a number of ternary chalcopyrite semiconductors with nearly the same physical and electronic structure as $AgGaTe_2$ that can be expected to give similarly beneficial Seebeck coefficients and isotropic electronic conductivity. To illustrate the point, in Fig. 8 we present the calculated band structure of *six* different chalcopyrite structure semiconductors, including $AgGaTe_2$. For simplicity we limit ourselves to the valence-band structure as most, if not all, of these compounds generally behave as p-type semiconductors. We note first that in all these compounds the valence-band maximum is centered at Γ (note that the plots are scaled so that within a given plot, momentum space distances between labeled points are essentially proportional to the distance along the x axis). The plots also indicate a general consistency of dispersive energy

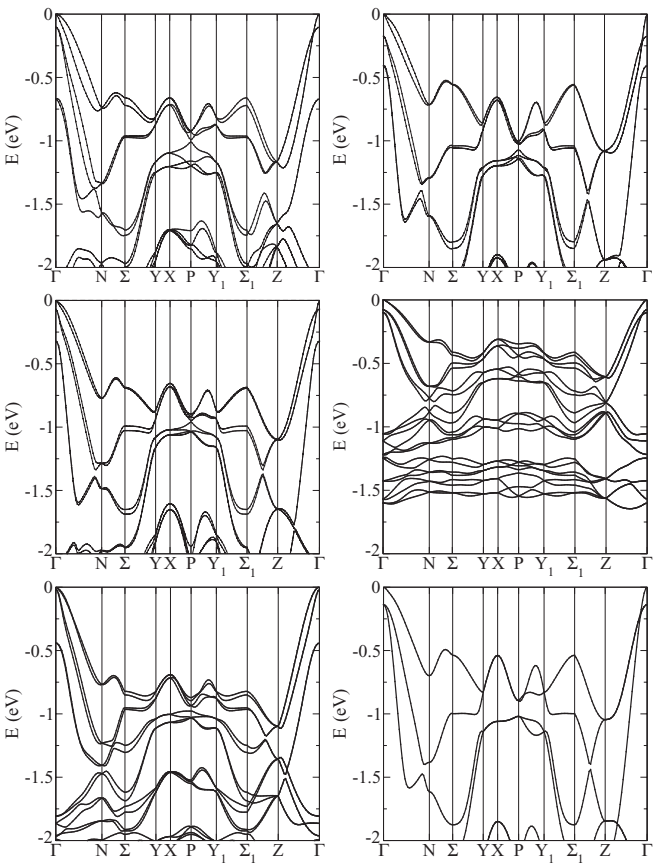

FIG. 8. The calculated valence-band structures of (top left) $AgGaTe_2$; top right $CdGeAs_2$; middle left $CdSnAs_2$; middle right $CuInS_2$; bottom left $CuInTe_2$; bottom right $ZnSiAs_2$.

TABLE I. Lattice thermal conductivity κ_{lattice} at 300 K and experimental band gaps of chalcopyrite compounds. Thermal conductivity (taken for polycrystalline samples) from Ref. 49, and band gaps from Ref. 52, except where noted.

Compound	κ_{lattice} (W/m K)	Band gap (eV)
$AgGaTe_2$	1.7 (Ref. 20)	1.15
$CdGeAs_2$	4.0	0.57
$CdSnAs_2$	7.5	0.26 (Ref. 50)
$CuInS_2$	12.5 (Ref. 51)	1.53
$CuInTe_2$	5.5	0.98
$ZnSiAs_2$	14.0	1.92

scales—for all of the plots the Γ-N dispersion is between 0.4 and 0.8 eV and that in the Γ-Z direction between 0.75 and 1.2 eV. While the plot-to-plot differences increase at greater distances (>1 eV) from the VBM, for the purposes of transport consideration these are of little importance.

As with $AgGaTe_2$, these valence-band plots generally contain a mixture of heavy and light bands. This has previously been shown[12,13] to be good for thermoelectric performance. However, the lattice thermal conductivity (presented in Table I) of most of these materials is much higher than that of $AgGaTe_2$, making them generally less favorable for thermoelectric performance. To the degree that this lattice term can be reduced by alloying and nanostructuring, these materials may show good performance as well. Given the large number of materials with very similar electronic structure, we would expect that alloying these materials with each other should be possible and effective at reducing κ_{lattice}. We note (Table I) that for these materials, with the exception of $CdSnAs_2$, the experimental band gap is sufficiently large to prevent bipolar conduction at temperatures below 900 K, so that the assessment of favorable valence-band structure implies good thermopower behavior as well.

Perhaps the likely best performer of the remaining five materials would be $CdGeAs_2$ with its 300-K lattice thermal conductivity listed in Ref. 49 as 4 W/m K. In Fig. 9 we present the calculated 900-K hole-doped thermopower (the melting point is 943 K) of this material, noting that even at the relatively high hole doping of 10^{20} cm^{-3} the thermopower is still over

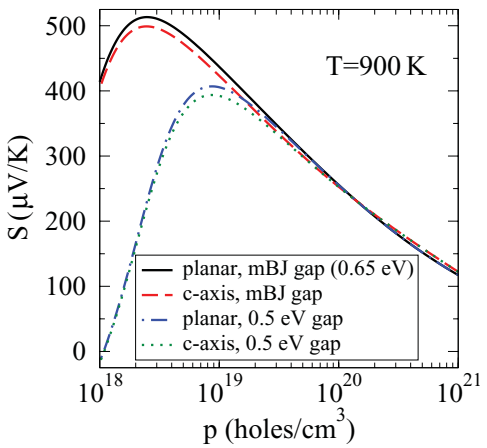

FIG. 9. (Color online) The calculated hole-doped thermopower of $CdGeAs_2$ at 900 K.

250 μV/K, an excellent value for thermoelectric performance, particularly since the lattice term at this temperature (assuming a canonical $1/T$ behavior) would be just 1.3 W/m K.

Included in the plot are two calculated curves—one assuming the first-principles calculated band gap of 0.65 eV, and a result assuming a somewhat smaller gap of 0.5 eV. We have included the additional curve because there is evidence[52] that the band gap of $CdGeAs_2$ decreases significantly with temperature. For both curves, as with the $AgGaTe_2$, the concentration dependence is essentially logarithmic at high dopings, until one approaches the bipolar regime where the thermopower decreases with decreasing concentration. For the as-calculated gap of 0.65 eV this happens for $p = 3 \times 10^{18}$ cm^{-3}; for the smaller gap this happens at 10^{19} cm^{-3}. Using the same criteria as for $AgGaTe_2$ we find that optimal doping will most likely be found for hole concentrations between 5×10^{19} and 2×10^{20} cm^{-3}, and this statement is independent of the value taken for the band gap. We note also that in the nonbipolar regime (i.e., to the right of the thermopower maximum in Fig. 9) the thermopower is very similar to that of $AgGaTe_2$, as would be expected given the similar electronic structure.

Although we have not calculated the thermopower of the remaining materials, to the extent that the dispersive energy scales are similar to those of $AgGaTe_2$ and $CdGeAs_2$ the thermopower will be similar as well. $CuInS_2$, in particular, may well have even larger thermopower than these materials given the smaller Γ -N and Γ-Z dispersions; actual performance of this material, however, is expected to be low due to the high lattice thermal conductivity and likely low mobility of this sulfide; the same considerations apply to $ZnSiAs_2$.

V. CONCLUSION

To conclude, in this work we have shown that the ternary chalcopyrite semiconductor $AgGaTe_2$ may show excellent thermoelectric performance at hole dopings ranging from 4×10^{19} and 2×10^{20} cm^{-3} at 900 K to between 2×10^{19} and 10^{20} cm^{-3} at 700 K. This performance may well be due to a heavy band–light band structure near the valence-band maximum and will be aided by nearly isotropic transport. In addition, we have shown that the valence-band structure of this material is very similar to that of a number of ternary chalcopyrite semiconductors, which might therefore show good thermoelectric performance if not for a relatively high lattice thermal conductivity. Given the general alloying capability of chalcopyrite semiconductors, it may be of interest to pursue heavy doping of these materials in concert with alloying with other chalcopyrite materials.

ACKNOWLEDGMENTS

D.J.S. is grateful for helpful discussions on tetrahedrally bonded thermoelectric materials with X. Shi, Lili Xi, Jiong Yang, and Wenqing Zhang. This research was supported by the US Department of Energy, EERE, Vehicle Technologies, Propulsion Materials Program (D.P.) and the Solid State Solar-Thermal Energy Conversion Center (S3 TEC), an Energy Frontier Research Center funded by the US Department of Energy, Office of Science, Office of Basic Energy Sciences under Award No. DE-SC0001299/DE-FG02-09ER46577 (D.J.S.).

APPENDIX: EXPLANATION OF FAVORABILITY OF HEAVY BAND–LIGHT BAND MIXTURE

In this section we give an explanation for the favorable thermoelectric properties of a heavy band–light band mixture. Consider a system with two parabolic bands of effective masses m_1 and m_2. For simplicity we will assume that they are degenerate in energy at the valence-band maximum, work at low temperature in which the Mott formula is valid, and consider the behavior of the power factor $S^2\sigma(T)$ in two relevant situations, relative to the case in which there is only a single band. To ensure a fair comparison these situations will be the following: the Fermi energy in the two-band case is the same as in the one-band case; and the carrier concentration in these two situations is the same. To begin, we recall the Mott formula, given as (neglecting factors of k_B,$\hbar$, and e, the electron charge)

$$S(T) = \frac{\pi^2}{3} T \left(\frac{d\sigma(E)/dE}{\sigma(E)} \right)_{|E=E_F}. \tag{A1}$$

We shall assume that the scattering time τ is constant throughout the following analysis. For a single parabolic band the logarithmic derivative in the previous expression reduces to $3/2E_F$, and a quick check reveals that this relationship holds in the case of *two* (or more) degenerate parabolic bands. This implies that in the situation wherein the two-band E_F is the same as the one band, the thermopower is unchanged, and since the electrical conductivities of the two bands add linearly the power factor is clearly enhanced by the addition of the extra band.

The second situation, in which carrier concentration is assumed to be the same in the single- and two-band cases, requires somewhat more work to analyze due to the change of the Fermi energy from the single-band case to the two-band case. Consideration of the $T = 0$ limit of the carrier concentration by integrating the density of states yields the following result, valid for two parabolic bands:

$$E_F = A \left(\frac{3n}{2} \right)^{2/3} \left[m_1^{3/2} + m_2^{3/2} \right]^{-2/3}, \tag{A2}$$

where A is a constant independent of carrier concentration, energy, or the masses. Similarly, for two parabolic bands the transport function can be written as

$$\sigma(E) = B E^{3/2} \left(m_1^{1/2} + m_2^{1/2} \right) \tag{A3}$$

with B a constant. Combining the previous two expressions in the low-temperature limit in which $E \to E_F$, we find that

$$\sigma(E_F) = C \frac{3n}{2} \frac{m_1^{1/2} + m_2^{1/2}}{m_1^{3/2} + m_2^{3/2}}. \tag{A4}$$

Here C is a constant independent of the band masses, temperature, and concentration. One may readily see, by imagining m_1 to be the mass in the single-band case, that if $m_2 < m_1$ the transport function and hence electrical conductivity *increase* via the addition of the second band, while the reverse is true if $m_2 > m_1$. This second result is made reasonable by considering that at fixed carrier concentration one is essentially asking about the effect of the second band on electrical *mobility*, and it is clear that if the second (degenerate in energy) band is heavier than the first the mobility will decrease.

It is possible to show, however, that even in this last case, and in fact regardless of the mass of the second band, the *power factor* $S^2\sigma(T)$ will increase as a result of the addition of the second band. To see this we write S, using the Mott relation for parabolic bands presented earlier, as

$$S(T) = \frac{\pi^2}{2} T / E_F \tag{A5}$$

and substitute previous expressions for E_F to find finally

$$S^2(T)\sigma(E_F) = D T^2 \left(\frac{2}{3n} \right)^{1/3} \left(m_1^{3/2} + m_2^{3/2} \right)^{1/3} \times \left(m_1^{1/2} + m_2^{1/2} \right), \tag{A6}$$

where D is a constant independent of the band masses, temperature, and concentration. In this expression the effect of m_2 is found to be an increase regardless of its value; the increase of $S^2(T)$ as a result of adding the second band, whether heavy or light, outstrips the decrease in mobility if $m_2 > m_1$, and is supported by an increase in mobility if $m_1 > m_2$. For simplicity we have here taken the electrical conductivity $\sigma(T)$ at low temperature to be $\sigma(E_F)$, the transport function evaluated at the zero-temperature Fermi energy, which holds in the same regime in which the Mott relation is valid. We note also that the above expression implies that for a given m_1, a larger m_2, signifying a heavier band, increases thermoelectric performance more than a band of the same mass would, suggesting the beneficial effect of heavier band mass. Finally, for sufficiently small doping the range of temperature in which the expressions for S and $\sigma(T)$ are valid shrinks rapidly. In particular, the power factor $S^2\sigma$ does *not* diverge as $n \to 0$, as implied by Eq. (A6), since one then approaches the nondegenerate limit [in which Pisarenko behavior, $S \sim -\log(n)$, applies] at arbitrarily low temperature.

It should be stated that all of these calculations assume that the electron relaxation time does not vary when either the Fermi energy or carrier concentration is held constant (as the second band is "added"), and the accuracy of this assumption can reasonably be debated. Therefore the previous argument should be considered as a plausible explanation for the observed behavior—the beneficial nature of heavy-light band structures—rather than as a rigorous argument proving that these band structures are good for thermoelectric performance.

[1] B. Poudel, Q. Hao, Y. Ma, Y. Lan, A. Minnich, B. Yu, X. Yan, D. Wang, A. Muto, D. Vashaee, X. Chen, J. Liu, M. S. Dresselhaus, G. Chen, and Z. Ren, Science **320**, 634 (2008).

[2] W. Xie, X. Tang, Y. Yan, Q. Zhang, and T. M. Tritt, Appl. Phys. Lett. **94**, 102111 (2009).

[3] B. C. Sales, D. Mandrus, and R. K. Williams, Science **272**, 1325 (1996).

[4] T. He, J. Chen, H. D. Rosenfeld, and M. A. Subramanian, Chem. Mater. **18**, 759 (2006).

[5]X. Shi, S. Bai, L. Xi, J. Yang, W. Zhang, L. Chen, and J. Yang, J. Mater. Res. **26**, 1745 (2011).
[6]L. D. Hicks and M. S. Dresselhaus, Phys. Rev. B **47**, 12727 (1993).
[7]H. Wang, Y. Pei, A. D. LaLonde, and G. J. Snyder, Adv. Mater. **23**, 1366 (2011).
[8]K. F. Hsu, S. Loo, F. Guo, W. Chen, J. S. Dyck, C. Uher, T. Hogan, E. K. Polychroniadis, and M. G. Kanatzidis, Science **303**, 818 (2004).
[9]G. J. Snyder and E. S. Toberer, Nat. Mater. **7**, 105 (2008).
[10]M. S. Dresselhaus, G. Chen, M. Y. Tang, R. G. Yang, H. Lee, D. Z. Wang, Z. F. Ren, J.-P. Fleurial, and P. Gogna, Adv. Mater. **19**, 1043 (2007).
[11]J. E. Jaffe and A. Zunger, Phys. Rev. B **30**, 741 (1984); **28**, 5822 (1983).
[12]D. J. Singh and I. I. Mazin, Phys. Rev. B **56**, R1650 (1997).
[13]A. F. May, D. J. Singh, and G. J. Snyder, Phys. Rev. B **79**, 153101 (2009).
[14]D. J. Singh, Phys. Rev. B **61**, 13397 (2000).
[15]D. J. Singh and D. Kasinathan, J. Electron. Mater. **36**, 736 (2007).
[16]H. J. Xiang and D. J. Singh, Phys. Rev. B **76**, 195111 (2007).
[17]K. Kuroki and R. Arita, J. Phys. Soc. Jpn. **76**, 083707 (2007).
[18]P. Wissgott, A. Toschi, G. Sangiovanni, and K. Held, Phys. Rev. B **84**, 085129 (2011).
[19]J. P. Heremans, V. Jovovic, E. S. Toberer, A. Saramat, K. Kurosaki, A. Charoenphakdee, S. Yamanaka, and G. J. Snyder, Science **321**, 554 (2008).
[20]A. Yusufu, K. Kurosaki, A. Kosuga, T. Sugahara, Y. Ohishi, H. Muta, and S. Yamanaka, Appl. Phys. Lett. **99**, 061902 (2011).
[21]P. Blaha, K. Schwarz, G. K. H. Madsen, D. Kvasnicka, and J. Luitz, WIEN2k, An Augmented Plane Wave + Local Orbitals Program for Calculating Crystal Properties (Karlheinz Schwarz, Techn. Universität Wien, Austria), 2001.
[22]F. Tran and P. Blaha, Phys. Rev. Lett. **102**, 226401 (2009).
[23]A. D. Becke and E. R. Johnson, J. Chem. Phys. **124**, 221101 (2006).
[24]J. P. Perdew, K. Burke, and M. Ernzerhof, Phys. Rev. Lett. **77**, 3865 (1996); **78**, 1396 (1997).
[25]G. K. H. Madsen, K. Schwarz, P. Blaha, and D. J. Singh, Phys. Rev. B **68**, 125212 (2003).
[26]J. M. Ziman, *Principles of the Theory of Solids* (Cambridge University Press, Cambridge, England, 1999).
[27]D. J. Singh, Phys. Rev. B **81**, 195217 (2010).
[28]D. Parker and D. J. Singh, Phys. Rev. B **82**, 035204 (2010).
[29]L. Zhang, M.-H. Du, and D. J. Singh, Phys. Rev. B **81**, 075117 (2010).
[30]K. P. Ong, D. J. Singh, and P. Wu, Phys. Rev. B **83**, 115110 (2011).
[31]G. K. H. Madsen, K. Schwarz, P. Blaha, and D. J. Singh, Phys. Rev. B **68**, 125212 (2003).
[32]D. J. Singh and I. I. Mazin, Phys. Rev. B **56**, R1650 (1997).
[33]T. J. Scheidemantel, C. Ambrosch-Draxl, T. Thonhauser, J. V. Badding, and J. O. Sofo, Phys. Rev. B **68**, 125210 (2003).
[34]L. Bertini and C. Gatti, J. Chem. Phys. **121**, 8983 (2004).
[35]L. Lykke, B. B. Iversen, and G. K. H. Madsen, Phys. Rev. B **73**, 195121 (2006).
[36]Y. Wang, X. Chen, T. Cui, Y. Niu, Y. Wang, M. Wang, Y. Ma, and G. Zou, Phys. Rev. B **76**, 155127 (2007).
[37]J. O. Sofo and G. D. Mahan, Phys. Rev. B **49**, 4565 (1994).
[38]D. Parker and D. J. Singh, New J. Phys. (in press).
[39]A. H. Reshak, Physica B **369**, 245 (2005).
[40]M. Lax, *Symmetry Principles in Solid State and Molecular Physics* (John Wiley, New York, 1974), p. 449; W. Setyawan and S. Curtarolo, Comp. Mat. Sci. **49**, 299 (2010).
[41]B. Tell, J. L. Shay, and H. M. Kasper, Phys. Rev. B **9**, 5203 (1974).
[42]R. Kumar and R. K. Bedi, J. Mater. Sci. **40**, 455 (2005).
[43]U. N. Roy, B. Mekonen, O. O. Adetunki, K. Chattopahhyay, F. Kochari, Y. Cui, A. Burger, and J. T. Goldstein, J. Cryst. Growth **241**, 135 (2002).
[44]P. G. Schunemann, S. D. Setzler, T. M. Pollak, M. C. Ohmer, J. T. Goldstein, and D. E. Zelmon, J. Cryst. Growth **211**, 242 (2000).
[45]S. Chatraphorn, T. Panmatarite, S. Pramatus, A. Prichavudhi, R. Kritayakirana, J. O. Berananda, V. Sayakanit, and J. C. Woolley, J. Appl. Phys. **57**, 1791 (1985).
[46]S. Arai, S. Ozaki, and S. Adachi, Appl. Opt. **49**, 829 (2010).
[47]B. R. Pamplin, T. Kiyowasa, and K. Masumoto, Prog. Cryst. Growth Charact. **1**, 331 (1979).
[48]J. Shewchun, J. J. Loferski, R. Beaulieu, G. H. Chapman, and B. K. Garside, J. Appl. Phys. **50**, 6978 (1979).
[49]D. P. Spitzer, J. Phys. Chem. Sol. **31**, 19 (1970).
[50]Our theoretical calculations find the band gap of this compound to be 0.44 eV, substantially larger than the experimental value.
[51]L. A. Makovetskaya, I. V. Bodnar, B. V. Korzun, and G. P. Yaroshevich, Phys. Status Solidi A **74**, K59 (1982).
[52]Landolt Börnstein Database, Springer Materials, available online at www.springermaterials.com.